Modern Chemistry
2026, Vol. 14, No. 2, pp. 71–78
https://doi.org/10.11648/j.mc.20261402.13

Research Article

Fabrication of Polymer Composites Materials Using Waste PP and Waste PET Bottles Filled with Sugarcane Bagasse Particles

Akilu Abdulrazak[1, *], Danladi Abdullahi[2], Bukhari Muhammad Musa[2], Wahid Muhd Haniff[3], Aliyu Auwal Jaji[4]

[1]Department of Pure and Applied Chemistry, Kaduna State University, Kaduna, Nigeria
[2]Department of Polymer and Textile Engineering, Ahmadu Bello University, Zaria, Nigeria
[3]Department of Chemistry, Universiti Putra, Selangor, Malaysia
[4]Department of Armament Engineering, Air Force Institute of Technology, Kaduna, Nigeria

Abstract

This study fabricated polymer composites from waste polyethylene terephthalate (PET) bottles and waste polypropylene (PP) using maleic anhydride MA to improve dispersion. The properties such as physical properties, mechanical properties and chemical properties of the polymer composites produced was identified, the physical properties shows that the density of the polymer composites was found to be 0.96g/cm^3, 1.04g/cm^3, 0.95g/cm^3 and 1.05g/cm^3 for sample Ab, Ac, Bb and Bc respectively as a result of filler dispersion, while the water absorption was found to be 5.12%,5.02%, 5.71% and 5.11% for sample Ab, Ac, Bb and Bc respectively due to the hydrophilic nature of the sugarcane bagasse particles. The mechanical properties results indicated that the inclusion of sugarcane bagasse particles produced a polymer composites with a good tensile strength of 22.93MPa, 25.47MPa, 25.07MPa, and elastic modulus of 28.80MPa, 284.96MPa, 287.04MPa, 289.96MPa and 200.79MPa for sample Ab, Ac, Bb and Bc respectively. The flexural strength of the polymer composites was found to be 37.45MPa, 39.91MPa, 41.50MPa and 49.41MPa for sample Ab, Ac, Bb and Bc respectively while the flexural modulus was found to be 760.8MPa, 804.7MPa, 847.2MPa and 956.5MPa. This was due to uniform dispersion of fine sugarcane bagasse particles and improved stress transfer at the matrix filler interfacial region promoted by maleic anhydride. The Fourier Transform Infrared Spectroscopy (FTIR) analysis affirmed chemical interactions between the polymer matrix and treated bagasse, with characteristic peaks corresponding to C=O stretching of PET and O–H groups of cellulose. The appearance of new peaks around 1730 cm^{-1} and the reduction in intensity of hydroxyl bands indicated esterification and enhanced compatibility through maleic anhydride coupling. The properties of the polymer composites produced is suitable for different application and also serves as plastic and agricultural waste management.

Keywords

Maleic Anhydride, Sugarcane Bagasse, Polymer Composites

*Correspondence: Akilu Abdulrazak (aabdulrazak08@gmail.com)

Received: 12 May 2026; **Accepted:** 20 May 2026; **Published:** 15 June 2026

1. Introduction

Plastics rank among the most commonly utilized materials worldwide due to their adaptability, strength, and relatively affordable production costs. Polyethylene terephthalate (PET) and polypropylene (PP) are some of the most frequently used types of plastics, appearing in products like packaging, clothing, car components, and household items. Nonetheless, their widespread application has risen significant environmental issues since these plastics do not break down naturally and pile up in nature, creating considerable challenges for managing solid waste [7]. Mixing various waste plastics, including PET and PP, offers a potential recycling solution. Nevertheless, PET and PP cannot easily mix because of their differing polarity and molecular structures, resulting in weak bonding between them and lower mechanical qualities in the mixture. [19] This lack of compatibility restricts their immediate application in structural and engineering fields. To address this issue, compatibilizers such as polymers that have been grafted with maleic anhydride are used to promote better adhesion between the materials and improve the overall qualities of the plastic blends. [12].

The use of natural fibers and fillers from agricultural waste in polymer materials has gained a lot of interest, in addition to making them compatible. These natural fillers are not only affordable but also renewable and good for the environment. One such filler is sugarcane bagasse, which is a plentiful by-product of the sugar-making process and is high in cellulose, hemicellulose, and lignin. When included in polymer composites, it can help lower material costs, make the materials biodegradable, and improve their physical, mechanical and chemical properties. [13]

This paper focuses on the fabrication of polymer composites using waste PET bottles and waste PP filled with sugarcane bagasse particles.

2. Methodology

2.1. Sample Preparation

To fabricate composites from waste PET, waste PP, and sugarcane bagasse that are made compatible with maleic anhydride, a two-roll mill was used for compounding, followed by compression molding according to the mass ratio in Table 1. Before the compounding process, all raw materials were treated and dried to remove moisture, ensuring they mixed evenly during processing. [17]

Table 1. *Formulation of compatibilized particles reinforced polymer composites.*

S/N	Designation	PETw (w%)	PPw (w%)	Sugarcane bagasse particles (w%)	Maleic anhydride (w%)
1	Ab	40	35	20	5
2	Ac	40	30	25	5
3	Bb	50	30	15	5
4	Bc	30	50	15	5

2.2. Density

The composites densities were determined in accordance with (ASTM D792-08). The volume of the composite was determined using length 50mm, width 50mm, thickness 5.0mm and the weight was measured using sensitive weighing balance. The densities were calculated accordingly using equation.

$$\text{Density} = \frac{mass}{volume}\ (\text{g/cm}^3)$$

2.3. Water Absorption

The process for measuring water absorption followed the guidelines set by ASTM D570. Samples were created with dimensions of 25.0 mm by 25.0 mm by 5.0 mm. The water absorption test involved fully submerging the samples in distilled water at room temperature for a period of 7 days. The amount of water absorbed was assessed by weighing the samples every 24 hours using a digital balance [15]. The calculation for the percentage of water absorption in the composite samples was done using the formula provided below;

$$\%\ \text{Water Absorbed} = \frac{W2-W1}{W1} X\ \ 100$$

2.4. Tensile Strength

The evaluation of tensile strength was performed according

to ASTM D-638. Dumbbell-shaped samples were placed under tensile force, and the machine automatically measured and reported the tensile strength, tensile modulus, and percentage elongation at break for each sample. These results were recorded on the certificate. [9].

2.5. Flexural Strength

The test for flexural strength on the mixtures followed ASTM D-790 standards. A sample, sized 100 mm x 25 mm x 3.2 mm, was set on two supports horizontally at an 80 mm distance. A constant force was then applied at the center using the loading nose, causing the sample to bend in a three-point manner until it ultimately broke. The highest load measured in Newtons and the related deflection in millimeters was noted as the sample broke. Using a formula, the flexural strength and flexural modulus were determined. [8]

$$\text{Flexural Strength} = 3FL/2bd2 \text{ (MPa)}$$

$$\text{Flexural Modulus} = FL3/4bd3D \text{ (MPa)}$$

Where F = Maximum Load at break, L = distance between the support spans at both edge of the specimen = 80mm, b = Sample width = 25mm, d = Sample thickness = 5.0 mm

2.6. Fourier Transform Infrared Spectroscopy (FTIR)

FTIR spectroscopy was employed to identify the functional groups present and to investigate the chemical interactions between the components of the composites. The analysis was performed using an FTIR spectrophotometer (Model PerkinElmer) over a wavelength range of 4000-400 cm^{-1} at a resolution of 4 cm^{-1}. The composite was ground into a fine powder, and a small amount was then placed directly onto the surface of the attenuated total reflectance ATR crystal. The spectra were each obtained by averaging 32 scans to improve the signal-to-noise ratio. The resulting spectra were analyzed to identify peaks corresponding to characteristic functional groups, chemical bonds, and possible interactions among PET, PP, maleic anhydride, and sugarcane bagasse components [3].

3. Results and Discussion

3.1. Density

Density measurements of the polymer composite samples reveal variations in structural tightness and internal arrangement resulting from the direct application of maleic anhydride in the PP/PET-sugarcane bagasse composite system. The lower density of sample Ab implies the presence of micro-voids and inefficient packing of the polymer matrix with lignocellulose particles. [4] This is often seen in natural fiber-reinforced polymer composites when the bonding at the interface is weak. In contrast, Sample Ac exhibits a higher density, which signifies improved compactness and reduced void space, resulting from enhanced interaction between the hydrophobic polymer matrix and hydrophilic sugarcane bagasse particles, facilitated by maleic anhydride. The density of Sample Bb is lower than anticipated, possibly resulting from inadequate wetting or the aggregation of fillers. In comparison, sample Bc exhibits the highest density, indicating superior packing efficiency, lower porosity, and greater compatibility within the composite system. The increase in density in this instance implies that there is robust bonding at the interface and enhanced structural integrity in the polymer composites modified with maleic anhydride. [11, 14].

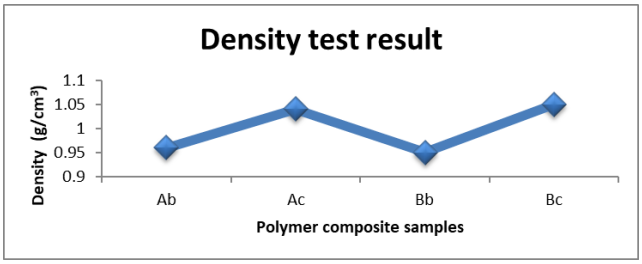

Figure 1. *Density of the polymer composites.*

3.2. Water Absorption

The water absorption properties of the composites are influenced by the bonding at the interfaces and the integrity of the microstructure. The sample Ab shows a moderate level of water absorption, which is believed to result from the presence of hydrophilic sites and micro-voids that enable water to penetrate. In contrast, sample Ac shows the lowest water absorption, indicating a denser composite structure with fewer pores, which implies better containment of sugarcane bagasse particles within the polymer matrix. The observed behavior indicates successful esterification and interfacial bonding, which is promoted by the direct incorporation of maleic anhydride. Sample Bb exhibits the highest water absorption, indicating greater porosity and increased exposure of hydrophilic fibre components, leading to enhanced moisture diffusion. In contrast, Sample Bc exhibits lower water absorption than Sample Bb, suggesting improved bonding at the interfaces and reduced water permeability. Previous research has shown that the incorporation of maleic anhydride in thermoplastic composites reinforced with natural fibres enhances fibre-matrix adhesion and reduces water uptake. [10, 15].

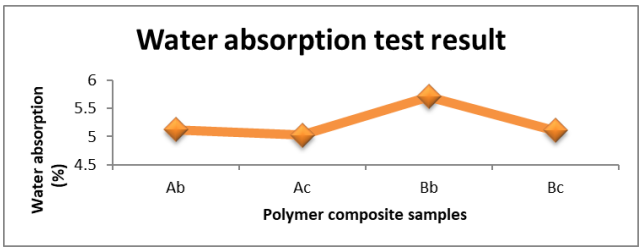

Figure 2. *Water absorption of polymer composites.*

3.3. Tensile Strength and Elastic Modulus

The tensile strength test results in Figure 3 demonstrate a gradual improvement in the composite samples, highlighting the beneficial effect of maleic anhydride on enhancing stress transfer within the composite system. The sample Ab exhibits the lowest tensile strength, suggesting poor adhesion at the interface and ineffective load transfer between the polymer matrix and sugarcane bagasse particles. Sample Ac exhibits higher tensile strength, indicating better adhesion at the interface and more effective reinforcement. Sample Bb exhibits a consistent tensile performance, signifying a stable ability to withstand loads during tensile deformation. Sample Bc's highest tensile strength indicates optimal bagasse particle dispersion and strong interfacial bonding facilitated by maleic anhydride, which enhances resistance to crack initiation and propagation. Research supports the importance of better interfacial compatibility in improving the tensile properties of fiber-reinforced polymer composites. The elastic modulus results shown in Figure 3 illustrate the stiffness behavior of the composites under tensile stress at [6] and [17]. Sample Ab exhibits relatively high stiffness, suggesting limited elastic deformation resulting from constrained polymer chain mobility. The modulus of Sample Ac shows a slight increase, suggesting more even load distribution between the matrix and reinforcement. The modulus value of Sample Bb remains consistent, indicating uniform stiffness throughout. In contrast, sample Bc exhibits a marked reduction in elastic modulus, indicating increased flexibility and ductility within the composite. The reduction in failure can be attributed to improved interfacial bonding and enhanced stress redistribution, enabling more elastic deformation before failure occurs. Enhanced interfacial compatibility in polymer composites has been observed to boost toughness at the expense of stiffness. [2, 5].

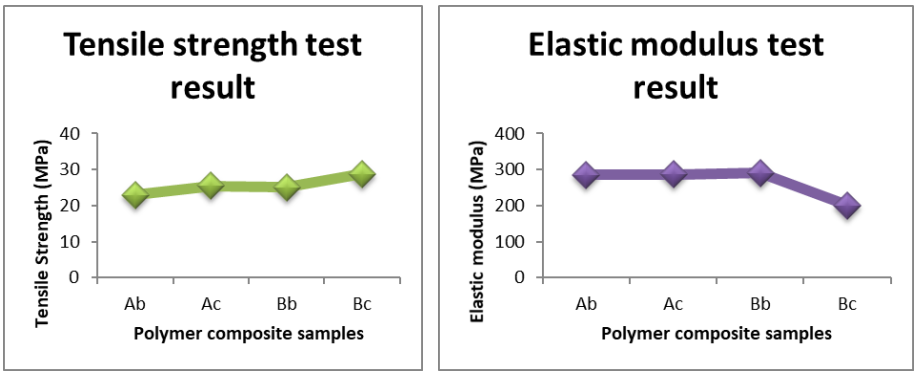

Figure 3. *Tensile strength and elastic modulus of the polymer composites.*

3.4. Flexural Strength and Flexural Modulus

Figure 4 shows a clear upward trend in flexural strength values from sample Ab to sample Bc, indicating improved resistance to bending stresses with a better composite formulation. Sample Ab exhibits the lowest flexural strength due to limited reinforcement efficiency and weak interfacial bonding under bending loads. The rise in sample Ac points to improved stress transfer and decreased interfacial slippage, due to the effect of maleic anhydride. Sample Bb shows a further increase in flexural strength, suggesting improved structural integrity and better filler distribution. Sample Bc exhibits the highest flexural strength, which is attributed to superior bending performance resulting from optimal interfacial adhesion, low void content, and efficient load transfer between the PP/PET matrix and sugarcane bagasse particles. Previous research has shown that maleic anhydride modification can significantly improve the flexural properties of natural fiber-reinforced polymer composites. Figure 4 illustrates the stiffness response of the composites under bending deformation, presenting the flexural modulus results for [1, 14]. Sample Ab displays the lowest flexural modulus, demonstrating a limited resistance to bending deformation. The flexural modulus of Sample Ac increases, suggesting improved stiffness as a result of enhanced interfacial bonding. The modulus in sample Bb increases further, demonstrating effective reinforcement and improved structural rigidity. Sample Bc exhibits the highest flexural modulus, indicating enhanced resistance to flexural deformation, which is attributed to strong interfacial bonding and effective stress transfer during bending. Enhanced fiber-matrix interaction

and uniform filler dispersion, as suggested by existing literature, notably boost flexural stiffness in polymer composites reinforced with lignocellulose fillers. [5]

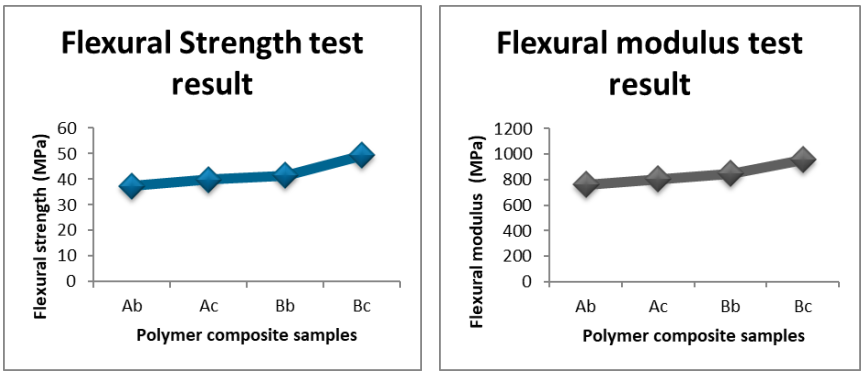

Figure 4. *Flexural strength and flexural modulus of the polymer composites.*

3.5. Fourier Transform Infrared Spectroscopy (FTIR)

The absorption spectrum of sample Ab, shown in Figure 5, displays a broad absorption band at approximately 3338 cm^{-1}, suggesting O–H stretching vibrations from hydroxyl groups in the cellulose of sugarcane bagasse, along with possible hydrogen bonding. Peaks at 2950 cm^{-1}, 2916 cm^{-1}, and 2849 cm^{-1} are notable, and are linked to C–H stretching vibrations, confirming the presence of an aliphatic polymer backbone. The peak at 1715 cm^{-1} is due to C=O stretching, whereas the peaks at 1236 cm^{-1} and 1097 cm^{-1} are attributed to C–O stretching vibrations in ester or ether groups. The persistence of the O–H band, accompanied by a slight shift in the C=O region, suggests the formation of intermolecular hydrogen bonds between the carbonyl groups of maleic anhydride and the hydroxyl groups of the bagasse filler. Previous reports have shown that maleic anhydride improves compatibility in natural fiber-polymer composites by forming ester or hydrogen-bonded connections. [9, 19] The spectrum for sample Ac, depicted in Figure 6 shows strong absorption bands at 2956 cm^{-1}, 2918 cm^{-1}, and 2848 cm^{-1}, reaffirming C–H stretching from the polypropylene (PP) and polyethylene terephthalate (PET) components. A distinct peak at 1714 cm^{-1} is associated with C=O stretching of ester or anhydride groups, consistent with the presence of PET and the compatibiliser (MA). The data implies that chemical compatibilization took place, thereby improving the interfacial adhesion between the hydrophilic fibre and the hydrophobic matrix, consistent with earlier research findings. [8]

The FTIR spectrum of sample Bb, depicted in Figure 7, displays characteristic absorption peaks at 2950 cm^{-1}, 2915 cm^{-1}, and 2848 cm^{-1}, which are indicative of the C–H stretching vibrations of aliphatic $–CH_2$ and $–CH_3$ groups, typical of polypropylene (PP) and polyethylene terephthalate (PET). A peak near 1715 cm^{-1} is assigned to the C=O stretching vibration of the ester carbonyl group in PET and potentially from the maleic anhydride (MA) group used as a compatibilizer. [18] Weak absorption bands between 1450 and 1370 cm^{-1} correspond to C–H bending vibrations, while the band around 1230 to 1090 cm^{-1} is due to C–O stretching in ester linkages. The peaks in the 700 to 900 cm^{-1} region are indicative of aromatic C–H out of plane bending modes, which confirms the aromatic character of PET. The absence of significant new peaks implies a physical blending of components, but the slight broadening near 1715 cm^{-1} and 1230 cm^{-1} may indicate weak chemical interactions or hydrogen bonding between maleic anhydride and the hydroxyl groups of sugarcane bagasse. [12]

Notable absorption peaks were observed in the Bc spectrum shown in Figure 8 at approximately 2948, 2915, and 2849 cm^{-1}, corresponding to the asymmetric and symmetric stretching vibrations of aliphatic C–H bonds in CH_2 and CH_3 groups. These bands are characteristic of the polypropylene backbone and indicate the presence of saturated hydrocarbon chains. [16]. A peak at approximately 1744 cm^{-1} is assigned to the stretching vibration of the carbonyl group from the ester linkage in PET, which serves as a key indicator of the polyester structure and verifies that PET retained its chemical structure within the composite. 3 The absorption bands at 1466 and 1376 cm^{-1} correspond to the bending vibrations of the CH_2 and CH_3 groups, respectively, while the peaks between 1258 and 1100 cm^{-1} are associated with C–O–C stretching vibrations in the ester groups of PET. Signals in the range of 972 to 841 cm^{-1} are attributed to C–H rocking and wagging modes characteristic of crystalline isotactic polypropylene. The weak absorption near 1100 cm^{-1} may indicate the presence of C–O stretching vibrations from cellulose and hemicellulose components of sugarcane bagasse fiber. [10] The detection of these cellulose-related peaks supports the integration of natural fibers into the composite structure.

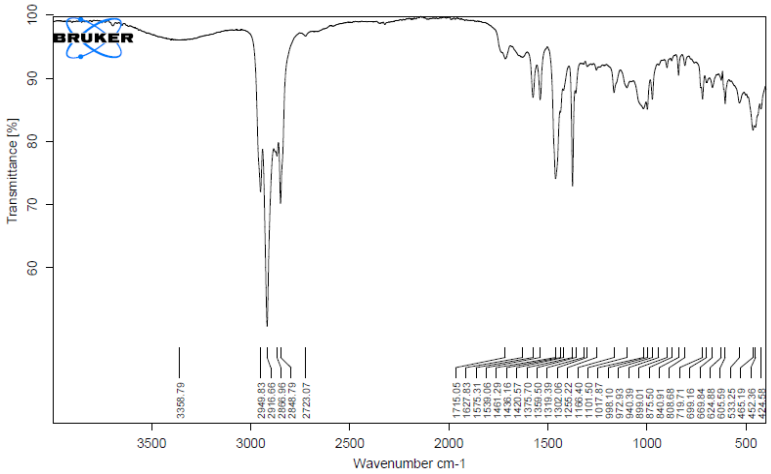

Figure 5. *FTIR spectrum of sample Ab.*

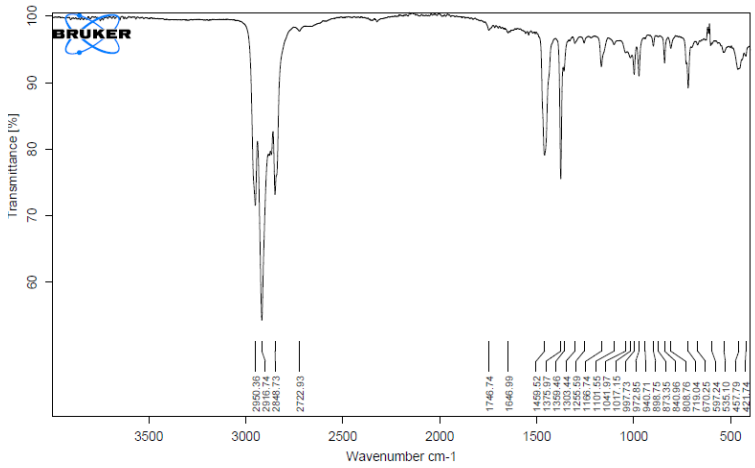

Figure 6. *FTIR spectrum of sample Ac.*

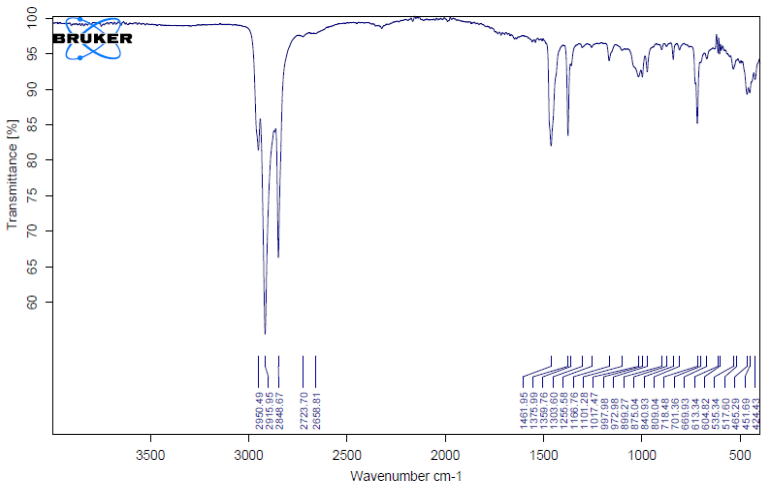

Figure 7. *FTIR spectrum of sample Bb.*

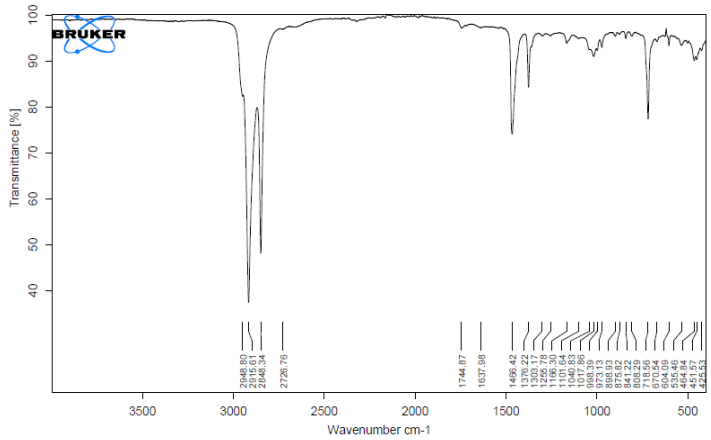

Figure 8. *FTIR spectrum of sample Bc.*

4. Conclusion

The research effectively demonstrated that waste PET and PP can be reinforced with sugarcane bagasse fibers to create high-performance and sustainable bio-composites. The use of maleic anhydride as a compatibilizer was crucial in enhancing the interfacial adhesion between the polymer matrix and the lignocellulose fibers. The improved chemical bonding observed in the FTIR spectra confirms the compatibilization process. Mechanical and physical testing showed that maleic anhydride significantly improved the structural integrity and resistance to deformation of the composite.

Abbreviations

PET	Polyethylene terephthalate
PETw	Waste Polyethylene terephthalate
PP	Polypropylene
PPw	Waste Polypropylene
MPa	Mega Pascal
MA	Maleic Anhydride

Author Contributions

Akilu Abdulrazak: Conceptualization
Danladi Abdullahi: Methodology
Bukhari Muhammad Musa: Formal Analysis
Wahid Muhd Haniff: Supervision
Aliyu Auwal Jaji: Resources

Conflicts of Interest

The authors declare no conflicts of interest.

References

[1] Bledzki, A. K., & Gassan, J. (1999). Composites reinforced with cellulose based fibres. Progress in Polymer Science, 24(2), 221–274. https://doi.org/10.1016/S0079-6700(98)00018-5

[2] Callister, W. D., & Rethwisch, D. G. (2020). Materials science and engineering: An introduction (10th ed.). Wiley.

[3] Coates, J. (2006). Interpretation of infrared spectra, a practical approach. In R. A. Meyers (Ed.), Encyclopedia of Analytical Chemistry (pp. 10815–10837). John Wiley & Sons.

[4] Faruk, O., Bledzki, A. K., Fink, H. P., & Sain, M. (2012). Biocomposites reinforced with natural fibers: 2000–2010. Progress in Polymer Science, 37(11), 1552–1596. https://doi.org/10.1016/j.progpolymsci.2012.04.003

[5] Fu, S. Y., Lauke, B., Mäder, E., Yue, C. Y., & Hu, X. (2008). Tensile properties of short-glass-fiber- and short-carbon-fiber-reinforced polypropylene composites. Composites Part A: Applied Science and Manufacturing, 39(6), 933–961. https://doi.org/10.1016/j.compositesa.2008.02.002

[6] George, J., Sreekala, M. S., & Thomas, S. (2001). A review on interface modification and characterization of natural fiber reinforced plastic composites. Polymer Engineering & Science, 41(9), 1471–1485. https://doi.org/10.1002/pen.10846

[7] Gupta, M. K., Srivastava, R. K., & Pathak, K. K. (2020). Chemical, mechanical, and thermal properties of polypropylene composites reinforced with rice husk, coir, and bagasse fibers. Journal of Thermoplastic Composite Materials, 33(10), 1397–1415.

[8] Haque, M. M., Islam, M. S., Huque, M. M., & Hasan, M. (2019). Mechanical properties of polypropylene composites reinforced with chemically treated coir and abaca fiber. Industrial Crops and Products, 141, 111773.

[9] Joseph, K., Thomas, S., & Pavithran, C. (2002). Effect of chemical treatment on the tensile properties of short sisal fiber-reinforced polyethylene composites. Composites Science and Technology, 59(11), 1625–1640. https://doi.org/10.1016/S0266-3538(99)00024-X

[10] Kabir, M. M., Wang, H., Lau, K. T., & Cardona, F. (2012). Chemical treatments on plant-based natural fibre reinforced polymer composites: An overview. Composites Part B: Engineering, 43(7), 2883–2892. https://doi.org/10.1016/j.compositesb.2012.04.053

[11] Ku, H., Wang, H., Pattarachaiyakoop, N., & Trada, M. (2011). A review on the tensile properties of natural fiber reinforced polymer composites. Composites Part B: Engineering, 42(4), 856–873. https://doi.org/10.1016/j.compositesb.2011.01.010

[12] Kumar, R., Raj, R. G., & Sinha, S. (2018). Effect of maleic anhydride on the mechanical and thermal properties of polypropylene composites reinforced with natural fibers. *Journal of Applied Polymer Science*, 135(1), 45672.

[13] Mishra, P., Singh, A., & Gupta, R. (2015). Influence of maleic anhydride compatibilization on mechanical and morphological behavior of hybrid natural fiber composites. *Journal of Applied Polymer Science*, 139(12), e51673.

[14] Pickering, K. L., Efendy, M. G. A., & Le, T. M. (2016). A review of recent developments in natural fibre composites and their mechanical performance. Composites Part A: Applied Science and Manufacturing, 83, 98–112. https://doi.org/10.1016/j.compositesa.2015.08.038

[15] Sreekala, M. S., Kumaran, M. G., & Thomas, S. (2002). Water sorption in oil palm fiber reinforced phenol formaldehyde composites. Composites Part A: Applied Science and Manufacturing, 33(6), 763–777. https://doi.org/10.1016/S1359-835X(02)00032-8

[16] Stuart, B. (2021). Infrared Spectroscopy: Fundamentals and Applications (2nd ed.). John Wiley & Sons.

[17] Thomason, J. L. (2009). The influence of fibre length, diameter and concentration on the modulus of glass fibre reinforced polypropylene. Composites Part A: Applied Science and Manufacturing, 40(8), 1141–1151. https://doi.org/10.1016/j.compositesa.2009.05.004

[18] Yang, H., Yan, R., Chen, H., Lee, D. H., & Zheng, C. (2012). Characteristics of hemicellulose, cellulose and lignin pyrolysis. Fuel, 86(12-13), 1781–1788.

[19] Zhang, X., Deng, Y., & Wang, L. (2014). Modification of natural fiber-reinforced composites with maleic anhydride and silane coupling agents. Polymer Composites, 35(2), 271–279.